

Optical study of OH radical in a wire-plate pulsed corona discharge

Wenchun Wang*, Su Wang, Feng Liu, Wei Zheng, Dezhen Wang

State Key Laboratory of Materials Modification by Laser, Ion and Electron beams, Dalian University of Technology,
Dalian 116024, PR China

Received 13 April 2005; accepted 11 May 2005

Abstract

In this study, the emission spectra of OH ($A^2\Sigma \rightarrow X^2\Pi$, 0–0) emitted from the high-voltage pulsed corona discharge (HVPCD) of N_2 and H_2O mixture gas and humid air in a wire-plate reactor were successfully recorded against a severe electromagnetic interference coming from HVPCD at one atmosphere. The relative vibrational populations and the vibrational temperature of N_2 (C, v') were determined. The emission spectra of the $\Delta v = +1$ (1–0, 2–1, 3–2, 4–3) vibration transition band of N_2 ($C^3\Pi_u \rightarrow B^3\Pi_g$) is simulated through gauss distribution. The emission intensity of OH ($A^2\Sigma \rightarrow X^2\Pi$, 0–0) has been exactly gotten by subtracting the emission intensity of the $\Delta v = +1$ vibration transition band of N_2 ($C^3\Pi_u \rightarrow B^3\Pi_g$) from the overlapping spectra. The relative population of OH ($A^2\Sigma$) has been obtained by the emission intensity of OH ($A^2\Sigma \rightarrow X^2\Pi$, 0–0) and Einstein's transition probability. The influences of pulsed peak voltage and pulse repetition rate on the relative population of OH ($A^2\Sigma$) radicals in N_2 and H_2O mixture gas and humid air are investigated separately. It is found that the relative population of OH ($A^2\Sigma$) rises linearly with increasing the applied peak voltage and the pulse repetition rate. When the oxygen is added in N_2 and H_2O mixture gas, the relative population of OH ($A^2\Sigma$) radicals decreases exponentially with increasing the added oxygen. The main involved physicochemical processes have also been discussed.

© 2005 Elsevier B.V. All rights reserved.

Keywords: OH Radicals; Emission spectrum; Pulsed corona discharge; Water vapor; Relative population

1. Introduction

Pulsed corona discharge is one of non-thermal plasma characterized by low gas temperature and high-electron temperature. By HVPCD, more electrical energy input goes into the production of energetic electrons than gas heating [1]. High-energy electrons (whose energy is in range of 5–20 eV) generated by HVPCD can efficiently dissociate, excite and ionize N_2 , O_2 and H_2O into oxygenated radicals (OH, HO_2 , O, H, etc.) or active species (O_3 , H_2O_2 , etc.) [2]. OH, O, H, N, HO_2 , N^+ , N_2^+ and O_3 , etc., active species with strong reactivity generated by HVPCD are considered important in removal of acid gases from flue gases, organic compounds removal from water, bacterial decontamination, VOCs decomposition and destruction of other toxic compounds, etc., fields [3–9]. Especially, OH radicals play the central role

for their strong oxidation in many physicochemical processes [10–11].

Recently, there have been a number of studies regarding the OH radicals [12–19]. Ono and Oda [12–15] had measured the OH radicals generated by a pulsed discharge by laser-induced fluorescence with a tunable KrF excimer laser and discussed the O radical's role to generate OH radical. Sun et al. [16] did some optical studies of active species (OH, O and H) produced by a pulsed streamer corona discharge in water. The influence of ultraviolet illumination on OH formation in dielectric barrier discharges (DBD) of Ar, O_2 and H_2O mixture was also studied [17]. Su et al. [18] introduced a new method by measuring the amount of CO_2 produced through oxidation of CO by OH radicals for the quantitative measurement of OH. Park et al. [19] investigated additive effect of C_2H_4 , H_2O , H_2O_2 on the emission intensity of OH and $NO/NO_2/NO_x$ reduction and analyzed the related reaction mechanism in corona discharge process using a wire-cylinder plasma reactor.

* Corresponding author. Tel.: +86 411 84709795–16;
fax: +86 411 84709304.

E-mail address: wangwenc@dlut.edu.cn (W. Wang).

In most of literatures, needle-plate or wire-cylinder is used as discharge electrode. In this article, we present the diagnostic results of OH ($A^2\Sigma \rightarrow X^2\Pi$, 0–0) emission spectra in HVPCD plasma with wire-plate electrode structure, which can produce more uniform corona discharge near the wires and is more close to industrial application. The emission spectra of the $\Delta v = +1$ (1–0, 2–1, 3–2, 4–3) vibration transition band of N_2 ($C^3\Pi_u \rightarrow B^3\Pi_g$) is simulated through gauss distribution. The emission intensity of OH ($A^2\Sigma \rightarrow X^2\Pi$, 0–0) has been exactly gotten by subtracting the emission intensity of the $\Delta v = +1$ vibration transition band of N_2 ($C^3\Pi_u \rightarrow B^3\Pi_g$) from the overlapping spectra. The relative population of OH ($A^2\Sigma$) has been obtained by the emission intensity of OH ($A^2\Sigma \rightarrow X^2\Pi$, 0–0) and Einstein's transition probability. The influences of peak voltage and pulse repetition rate on the relative population of OH ($A^2\Sigma$) radicals in N_2 and H_2O mixture gas and humid air are investigated under severe electromagnetic interference caused by HVPCD itself at one atmosphere. When the oxygen is added in N_2 and H_2O mixture gas, the varying of the relative population of OH ($A^2\Sigma$) radicals is investigated. The main involved physicochemical processes have also been discussed.

2. Experimental setup

The experimental setup is illustrated schematically in Fig. 1. It is composed of a pulsed power supply, a discharge reactor, an optical detection system and a gas-mixing chamber. The power supply including charge and discharge circuit is mainly composed of a DC high-voltage unit, a pulse generator and a spark gap. The pulsed power can supply

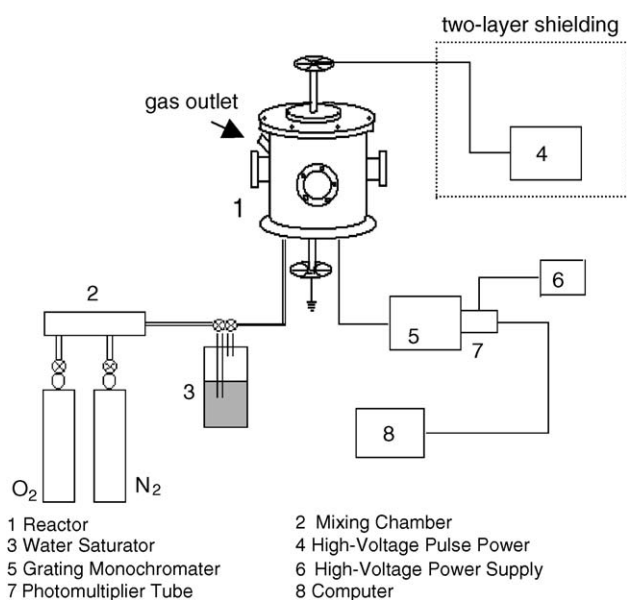


Fig. 1. Schematic of the experimental setup.

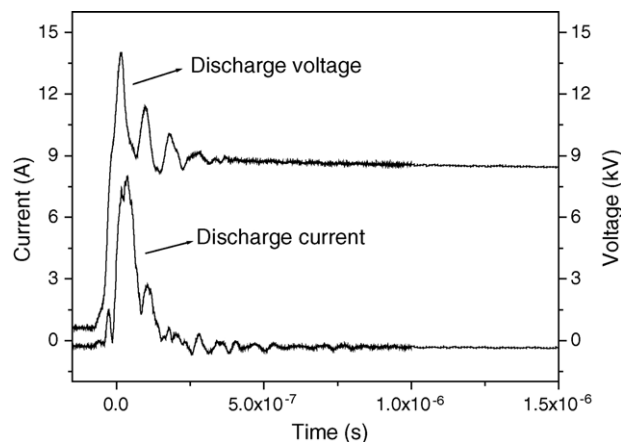


Fig. 2. Typical waveforms of discharge voltage and discharge current in N_2 and H_2O mixture.

high-voltage pulse with a rising time of 40 ns, a pulse width of about 500 ns and an adjustable repetition rate in range of 0–200 Hz. The discharge voltage is measured with an oscilloscope (Tektronix TDS3052B) and a 1:1000 high-voltage probe (Tektronix P6015A $1000 \times 3.0\text{pF}$ $100\text{M}\Omega$). The discharge current is measured with a current probe (Tektronix TCP202). Fig. 2 shows the waveforms of a discharge voltage and current. The pulsed corona discharge was generated in a stainless-steel chamber so that the environmental conditions could be controlled. The discharge chamber could be evacuated with a rotary pump. The reactor utilizes wire-plate electrode of which can be the 5–30 mm adjustable thick gas spacing, the stainless-steel wire-plate electrode is placed in the center of a stainless-steel chamber and the discharge plasma is produced in the gas spacing. A stainless steel plane (56 mm \times 56 mm) forms the grounded electrode. The positive high-voltage corona stainless steel wire, 48 mm long, 0.2 mm in diameter and 20 mm in space between each wire, is fixed 8 mm apart from the cathode plate. A quartz optical fiber head was parallelly placed to the wire electrode. In order to reduce the interference of discharge pulses to the detection system and other instruments, the high-voltage pulse power supply is placed in a two-layer shielding box. Both the pulsed power supply and the reactor are connected to the ground separately. The optical emission from the discharge region is collected by a MODEL SP-305 grating monochromator (grating groove is 1200 lines/mm, glancing wavelength is 350 nm). After the diffraction of the grating, the output spectral light is converted into an electrical signal by a photo multiplication tube (mode R928) and the output of the PMT is recorded by a computer. High purity N_2 (99.999%) and High purity O_2 (99.999%) are used as discharge gases under the gas pressure of 1.013×10^5 Pa. The N_2 bubbles the water to control humidity. The temperature of the water is heated at 100°C . When the N_2 bubbles through the water and uniformly diffuses into the discharge space, the gas temperature is about 80°C . The water vapor concentration is about 10% in discharge chamber.

3. Experimental results and discussion

3.1. The measurement of the OH radical emission spectra

In the non-equilibrium plasma generated by HVPCD at one atmospheric pressure, electrons with much bigger migration rates can be speeded up to 2–20 eV in kinetic energy [20]. The non-elastic collisions of the energetic electrons with H₂O, N₂ and O₂ molecules will induce H₂O, N₂ and O₂ molecules to be dissociated, excited and ionized. The radicals and active species of OH, HO₂, O, H, N, O₃, H₂O₂, O₂⁻, N⁺ and N₂⁺, etc., can be produced. Fig. 3A shows a typical emission spectrum produced by a positive pulsed corona discharge of N₂ and H₂O mixture at one atmosphere, 24 kV peak voltage and 40 Hz pulse repetition rate. The emission spectrum consists mainly of OH (A²Σ → X²Π, 0–0) and N₂ (C³Π_u → B³Π_g 1–0, 315 nm).

3.2. The relative vibrational population and the vibrational temperature of N₂ (C, v')

From Fig. 3A, we can see that the emission spectrum of OH (A²Σ → X²Π, 0–0) is seriously interfered by the

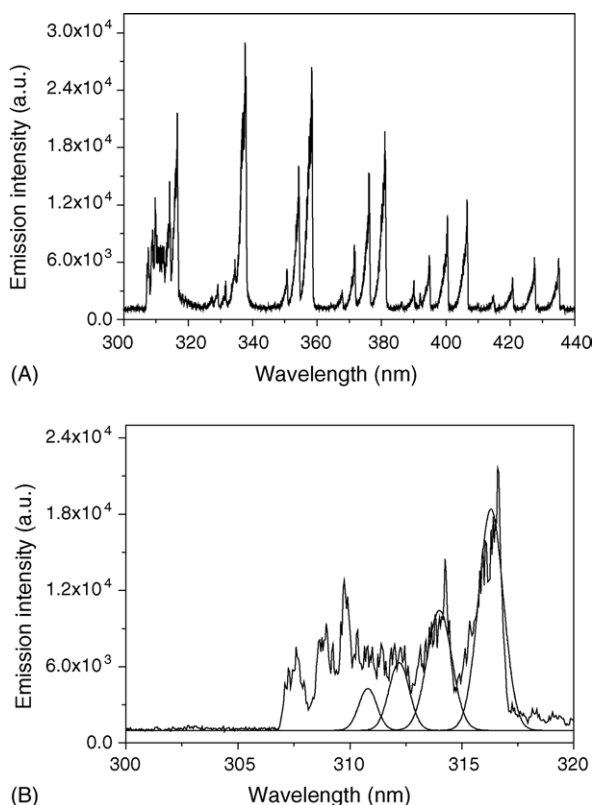


Fig. 3. (A) Typical emission spectrum of OH (A²Σ → X²Π, 0–0) and N₂ (C³Π_u → B³Π_g) generated by pulsed corona discharge in N₂ and H₂O mixture at 24 kV peak voltage and 40 Hz pulse repetition rate. (B) The emission intensity of OH (A²Σ → X²Π, 0–0) obtained through the simulation of the emission spectra of the Δv = +1 vibration transition band of N₂ (C³Π_u → B³Π_g) by the Gauss profile and the relative populations of N₂ (C, v').

emission spectrum of the Δv = +1 vibration transition band of N₂ (C³Π_u → B³Π_g). Therefore, it is necessary to subtract the emission intensity of the Δv = +1 vibration transition band of N₂ (C³Π_u → B³Π_g) from the overlapping spectra to get the emission intensity of OH (A²Σ → X²Π, 0–0). The relative vibrational population of N₂ (C, v') can be determined through the Eq. (1):

$$S_{v'v''} \propto N_{v'}(\text{FC})_{v'v''} R_e^2(r_{v'v''}) \nu_{v'v''}^3 \quad (1)$$

where $S_{v'v''}$ is the integral emission intensity, $N_{v'}$ the population of the electronic excitation state vibrational energy level v' , $(\text{FC})_{v'v''}$ the corresponding Frank–Condon factor, $R_e(r_{v'v''})$ the electronic transition moment and $R_e(r_{v'v''})$ is nearly constant, $\nu_{v'v''}$ is the corresponding transition frequency. By calculating the integral emission intensity $S_{v'v''}$ of the Δv = -3 and the Δv = -4 vibration transition bands of N₂ (C³Π_u → B³Π_g), the relative vibrational population of N₂ (C, v') in present experimental condition can be determined $N_0:N_1:N_2:N_3:N_4 = 1.00:0.352:0.135:0.063:0.031$ by Eq. (1). And then the vibrational temperature of N₂ (C) can be determined by the following equation:

$$\frac{N_1}{N_0} = e^{-\Delta E/kT_v} \quad (2)$$

where N_1 and N_0 is the relative vibrational population of the 1 and 0 vibrational states, respectively. ΔE is the energy difference between the 1 and 0 vibrational states and k is the Boltzman's constant. T_v stands for the vibrational temperature. Therefore, the vibrational temperature between the 1 and 0 vibrational states can be determined, and the vibrational temperatures between the 2 and 1, 3 and 2, 4 and 3 vibrational states also can be determined with the same method. At our present experimental conditions, the mean vibrational temperature of N₂ (C) is 2616.3 K.

The emission intensity of the Δv = +1 (1–0, 2–1, 3–2, 4–3) vibration transition band of N₂ (C³Π_u → B³Π_g) can be determined by Eq. (1) with the relative vibrational population of N₂ (C, v'), Frank–Condon factor and the spectrum response of photomultiplier tube. Since the experimental pressure is at one atmosphere, gas molecule collision frequency is about 10¹⁰ times per second by gas dynamics. The radiation lifetime of the N₂ (C) state is about 40 ns, therefore the N₂ (C) molecules collide with gas molecules about 400 times in a second. The rotational equilibrium is reached in each vibrational state of the N₂ (C) state, and then the vibrational distribution can be described by the same expression. Due to the difficulty of determining the exact emission spectrum line shape function, a Gaussian form was used for the deconvolution of the overlapping emission spectrum (Fig. 3B). The emission spectra of the Δv = +1 (1–0, 2–1, 3–2, 4–3) vibration transition band of N₂ (C³Π_u → B³Π_g) can be deduced quite accurately from the simulation process. And then the emission intensity of OH (A²Σ → X²Π, 0–0) can be exactly get by subtracting the emission intensity of the Δv = +1 vibration transition band of N₂ (C³Π_u → B³Π_g) from the overlapping spectra.

The relation between the emission intensity S and the excited state relative population is given as follows:

$$S = NAh\nu \quad (3)$$

where A is the Einstein's transition probability, h the Planck constant and ν is the transition frequency. Therefore, the relative population of OH ($A^2\Sigma$) can be determined by Eq. (3) with the emission intensity of OH ($A^2\Sigma \rightarrow X^2\Pi$, 0–0) and the corresponding Einstein's transition probability ($A(\text{OH}) = 0.0145 \times 10^8 \text{ s}^{-1}$).

3.3. The effects of peak voltage and frequency on the relative population of OH ($A^2\Sigma \rightarrow X^2\Pi$, 0–0)

When the wire-plate electrode is placed in air, the N_2 and H_2O mixture gas uniformly diffuse into the discharge area at the same flux and experimental conditions with Fig. 3A. The emission spectrum produced by a positive pulsed corona discharge is recorded as shown in Fig. 4.

It can be seen that the emission intensities of OH ($A^2\Sigma \rightarrow X^2\Pi$, 0–0) and N_2 ($C^3\Pi_u \rightarrow B^3\Pi_g$) in Fig. 3A are much larger than those in Fig. 4. Some mechanisms for the differences are discussed in the following:

- (1) In Fig. 4, there are some of O_2 in air. The concentration of N_2 in Fig. 4 is lower than that in Fig. 3A in discharge space. Therefore, the emission intensity of N_2 ($C^3\Pi_u \rightarrow B^3\Pi_g$) in Fig. 4 is certainly weaker than that in Fig. 3A.
- (2) The O_2 capture a large numbers of electrons in Fig. 4 and becomes negative ions. So the densities of the electrons in Fig. 4 are much lower than that in Fig. 3A under the same discharge conditions. The emission intensity of OH ($A^2\Sigma \rightarrow X^2\Pi$, 0–0) and N_2 ($C^3\Pi_u \rightarrow B^3\Pi_g$) is obviously weakened by the oxygen component of air in Fig. 4.

Fig. 5 clearly shows that the relative population of OH ($A^2\Sigma \rightarrow X^2\Pi$, 0–0) of N_2 and H_2O mixture gas and humid

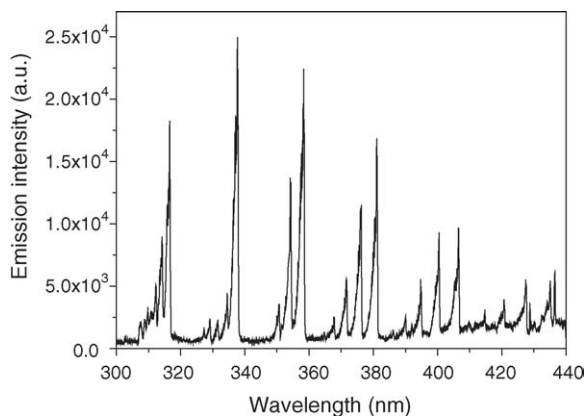


Fig. 4. Typical emission spectrum of OH ($A^2\Sigma \rightarrow X^2\Pi$, 0–0) and N_2 ($C^3\Pi_u \rightarrow B^3\Pi_g$) generated by pulsed corona discharge in humid air at 24 kV peak voltage and 40 Hz pulse repetition rate.

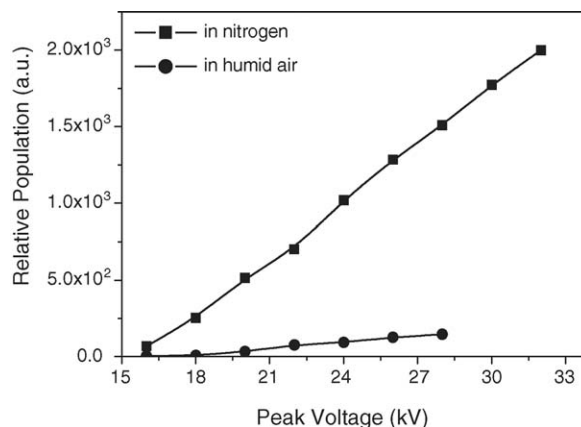


Fig. 5. The relative population of OH ($A^2\Sigma$) as a function of peak voltage at one atmosphere and 40 Hz discharge repetition rate.

air vary as a function of peak voltage. The repetition rate of pulsed discharge is 40 Hz and is kept constant during the measurements. The flow rate of N_2 into the reactor is kept at 200 ml/min. From Fig. 5, we can see that the relative population of OH ($A^2\Sigma \rightarrow X^2\Pi$, 0–0) increase linearly with increasing peak voltage.

OH radicals are mainly produced by electron–molecule collision process. The reaction is as follows:



Because a higher peak voltage can cause an increase in the high-energy electron density and the electron mean energy, the relative population of OH ($A^2\Sigma \rightarrow X^2\Pi$, 0–0) increases linearly with peak voltage.

The effect of pulse repetition rate on the relative population of OH ($A^2\Sigma \rightarrow X^2\Pi$, 0–0) is shown in Fig. 6. The power supply voltage is 20 kV and is kept constant during the measurements. The flow rate of N_2 into the reactor is kept at 200 ml/min. From Fig. 6, we can see that the relative population of OH ($A^2\Sigma \rightarrow X^2\Pi$, 0–0) increase linearly with increasing repetition rate of pulsed discharge. For the peak voltage is not changed, per unit pulse discharge creates the nearly same number of radicals and active species. Thus

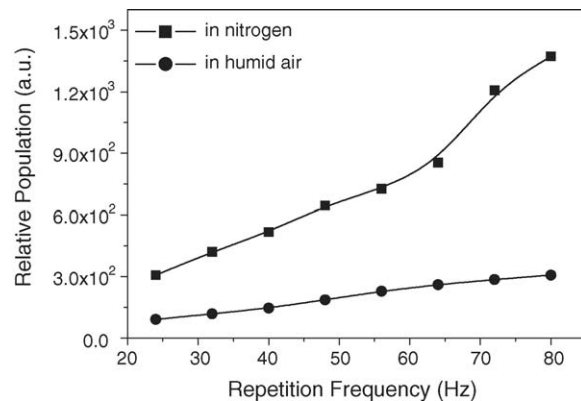


Fig. 6. The relative population of OH ($A^2\Sigma$) as a function of discharge repetition rate at one atmosphere and 20 kV peak voltage.

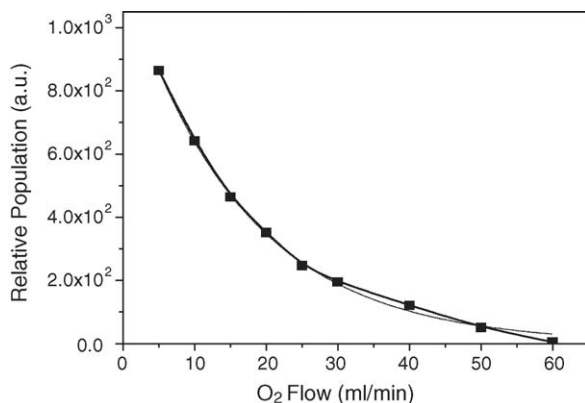


Fig. 7. The relative population of OH ($A^2\Sigma$) as a function of O_2 flow rate at 24 kV peak voltage and 40 Hz repetition rate. The solid line is experimental curve. The dot line is obtained by the exponential fitting method.

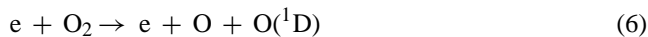
the relative population of OH ($A^2\Sigma \rightarrow X^2\Pi$, 0–0) increase linearly with increasing pulse repetition rate.

3.4. The Effects of O_2 addition on the relative population of OH ($A^2\Sigma \rightarrow X^2\Pi$, 0–0)

To investigate the effect of oxygen on the relative population of OH ($A^2\Sigma \rightarrow X^2\Pi$, 0–0), oxygen is added in the N_2 and H_2O mixture in positive pulsed corona discharge. When oxygen is added, the added O_2 capture a lot of free electrons and form O_2^- ions. Thus, the added O_2 decrease greatly the density of free electrons and the electron mean energy.

The effects of the concentration of O_2 on the relative population of OH ($A^2\Sigma$) are shown in Fig. 7. Fig. 7 clearly shows that the relative population of OH ($A^2\Sigma$) varies as a function of O_2 flow rate at 9 different oxygen flow rates of 5, 10, 15, 20, 25, 30, 40, 50 and 60 ml/min at 24 kV peak voltage and 40 Hz pulse repetition rate. The flow rate of N_2 into the reactor is kept at 200 ml/min. It can be seen that the relative population of OH ($A^2\Sigma$) is in the exponentially decreasing with the flow rate of oxygen.

In order to explain the observed experimental phenomena, we will further discuss the physicochemical processes of interaction when oxygen is added. Firstly the added O_2 can be dissociation by the reactions (5)–(7) in the electron–molecule interactions of electrons and O_2 :



A lot of $O(^1D)$ and O atoms can be produced. One and Oda [14] have pointed out that in a humid air, most of the OH can be produced by interaction of $O(^1D)$ and H_2O :



At the same time, the lots of O atoms and O_3 molecules produced by the added O_2 can react with OH and then decrease

OH ($A^2\Sigma$) greatly.



Because of the depletion of the OH radicals and the free electrons, the relative population of OH ($A^2\Sigma$) is decreasing with the added oxygen.

For further understanding of the observed phenomena and the mechanism involved, a detailed kinetic simulation of the HVPCD plasma is underway and will be reported later.

4. Conclusions

In this study, we have successfully recorded the emission spectra of OH ($A^2\Sigma \rightarrow X^2\Pi$, 0–0) in the positive pulse corona discharge with wire-plane electrode at one atmosphere. The severe electromagnetic interference caused by HVPCD itself has been overcome by double shielding and specially designed multiple grounding of the discharge source and the reactor. The relative vibrational populations and the vibrational temperature of N_2 (C , v') were determined. The emission spectra of the $\Delta v = +1$ (1–0, 2–1, 3–2, 4–3) vibration transition band of N_2 ($C^3\Pi_u \rightarrow B^3\Pi_g$) is simulated through gauss distribution. The emission intensity of OH ($A^2\Sigma \rightarrow X^2\Pi$, 0–0) has been exactly gotten by subtracting the emission intensity of the $\Delta v = +1$ vibration transition band of N_2 ($C^3\Pi_u \rightarrow B^3\Pi_g$) from the overlapping spectra. The relative population of OH ($A^2\Sigma$) has been obtained by the emission intensity of OH ($A^2\Sigma \rightarrow X^2\Pi$, 0–0) and Einstein's transition probability. It is found that the relative population of OH ($A^2\Sigma$) increase linearly with the peak voltage and the pulse repetition rate in N_2 and H_2O mixture gas and humid air. When the different oxygen flows are added in N_2 and H_2O mixture gas, the relative population of OH ($A^2\Sigma$) radicals decreases exponentially with increasing the flow rate of oxygen.

Acknowledgements

The author would like to thank professor Xuechu Li for friendly discussion and suggestion. This work is supported by the united fund of the National Natural Science Foundation Committee of China and Engineering Physical Institute of China granted under No. 10276008 and the fund of Liaoning Province Natural Science Foundation Committee granted under No. 20022138.

References

- [1] A. Mizuno, J.S. Clements, R.H. Davis, IEEE Trans. Ind. Appl. 22 (1986) 516.
- [2] R.P. Dahiya, S.K. Mishra, A. Veefkind, IEEE Trans. Plasma Sci. 21 (1993) 346.

- [3] A.T. Sugiarto, S. Ito, T. Ohshima, M. Sato, J.D. Skalny, J. Electrostatics 58 (2003) 135.
- [4] A. Abou-Ghazala, S. Katsuki, K.H. Schoenbach, F.C. Dobbs, K.R. Moreira, IEEE Trans. Plasma Sci. 30 (2002) 1449.
- [5] M. Yamamoto, M. Nishioka, M. Sadakata, J. Electrostatics 56 (2002) 173.
- [6] T. Oda, J. Electrostatics 57 (2003) 293.
- [7] U. Roland, F. Holzer, F.D. Kopinke, Catal. Today 73 (2002) 315.
- [8] G.W. Shao, J. Li, W.L. Wang, Z.H. He, S.L. Li, J. Electrostatics 62 (2004) 1.
- [9] H. Lin, X. Gao, Z.Y. Lou, K.F. Cen, M.X. Pei, Z. Huang, Fuel 83 (2004) 1251.
- [10] V.A. Lozovsky, I. Derzy, S. Cheskis, Chem. Phys. Lett. 284 (1998) 407.
- [11] A.A. Joshi, B.R. Locke, P. Arce, W.C. Finney, J. Hazard. Mater. 41 (1995) 3.
- [12] R. Ono, T. Oda, IEEE Trans. Ind. Appl. 37 (3) (2001) 709.
- [13] R. Ono, T. Oda, IEEE Trans. Ind. Appl. 36 (1) (2000) 82.
- [14] R. Ono, T. Oda, Thirty-Fourth IAS Annual Meeting, Industry Applications Conference, Conference Record of the 1999 IEEE, vol. 3, 1999, p. 1461.
- [15] R. Ono, T. Oda, J. Phys. D: Appl. Phys. 35 (2002) 2133.
- [16] B. Sun, M. Sato, J.S. Clements, J. Electrostatics 39 (3) (1997) 189.
- [17] Z. Falkenstein, J. Appl. Phys. 81 (11) (1997) 7158.
- [18] Z. Su, H.H. Kim, M. Tsutsui, K. Takashima, A. Mizuno, Thirty-Fourth IAS Annual Meeting, Industry Applications Conference, Conference Record of the 1999 IEEE, vol. 3, 1999, p. 1473.
- [19] C.W. Park, J.W. Hahn, D.N. Shin, The Pacific Rim Conference on Lasers and Electro-Optics, CLEO/Pacific Rim '1999, vol. 2, 1999, p. 356.
- [20] B. Eliasson, U. Kogelschatz, J. Phys. B: At. Mol. Phys. 19 (1986) 1241.